

Porphyrin-Based SOD Mimic MnTnBuOE-2-PyP⁵⁺ Inhibits Mechanisms of Aortic Valve Remodeling in Human and Murine Models of Aortic Valve Sclerosis

Wanda Anselmo, PhD;* Emanuela Branchetti, PhD;* Juan B. Grau, MD; Gen Li, PhD; Salma Ayoub, PhD; Eric K. Lai, MS; Nancy Rioux, RN; Artak Tovmasyan, PhD; Jacqueline H. Fortier, MSc; Michael S. Sacks, PhD; Ines Batinic-Haberle, PhD; Stanley L. Hazen, MD, PhD; Robert J. Levy, MD; Giovanni Ferrari, PhD

Background—Aortic valve sclerosis (AVSc), the early asymptomatic presentation of calcific aortic valve (AV) disease, affects 25% to 30% of patients aged >65 years. In vitro and ex vivo experiments with antioxidant strategies and antagonists of osteogenic differentiation revealed that AVSc is reversible. In this study, we characterized the underlying changes in the extracellular matrix architecture and valve interstitial cell activation in AVSc and tested in vitro and in vivo the activity of a clinically approved SOD (superoxide dismutase) mimic and redox-active drug MnTnBuOE-2-PyP⁵⁺ (BMX-001).

Methods and Results—After receiving informed consent, samples from patients with AVSc, AV stenosis, and controls were collected. Uniaxial mechanical stimulation and in vitro studies on human valve interstitial cells were performed. An angiotensin II chronic infusion model was used to impose AV thickening and remodeling. We characterized extracellular matrix structures by small-angle light scattering, scanning electron microscopy, histology, and mass spectrometry. Diseased human valves showed altered collagen fiber alignment and ultrastructural changes in AVSc, accumulation of oxidized cross-linking products in AV stenosis, and reversible expression of extracellular matrix regulators ex vivo. We demonstrated that MnTnBuOE-2-PyP⁵⁺ inhibits human valve interstitial cell activation and extracellular matrix remodeling in a murine model (C57BL/6J) of AVSc by electron microscopy and histology.

Conclusions—AVSc is associated with architectural remodeling despite marginal effects on the mechanical properties in both human and mice. MnTnBuOE-2-PyP⁵⁺ controls AV thickening in a murine model of AVSc. Because this compound has been approved recently for clinical use, this work could shift the focus for the treatment of calcific AV disease, moving from AV stenosis to an earlier presentation (AVSc) that could be more responsive to medical therapies. (*J Am Heart Assoc.* 2018;7:e007861. DOI: 10.1161/JAHA.117.007861.)

Key Words: aortic valve stenosis • extracellular matrix • reactive oxygen species • valve • valve interstitial cells

Aortic valve sclerosis (AVSc), the early presentation of calcific aortic valve disease (CAVD), is a hallmark of several cardiovascular conditions including congestive heart failure, myocardial infarction, and severe aortic valve stenosis (AS).^{1–5} Several clinical trials have failed to halt the development of CAVD, rendering this condition as treatable only at the end stages, through surgical or percutaneous means.^{6–9}

Sclerosis presents in 25% to 30% of patients aged >65 years and in up to 40% of those aged >75 years. It is characterized by thickening of the aortic valve (AV) leaflets with marginal effects on the mechanical properties of the valve, making its presentation largely asymptomatic.^{1,10,11} Of these patients, 10% will develop symptomatic AS within a decade. AS inevitably leads to heart failure and death unless patients

From the University of Pennsylvania, Philadelphia, PA (W.A., E.B., E.K.L.); Ottawa Heart Institute, Ottawa, Ontario, Canada (J.B.G., J.H.F.); Columbia University, New York, NY (G.L., G.F.); Texas University at Austin, TX (S.A., M.S.S.); The Valley Hospital, Ridgewood, NJ (N.R.); Duke University School of Medicine, Durham, NC (A.T., I.B.-H.); Cleveland Clinic, Cleveland, OH (S.L.H.); The Children's Hospital of Philadelphia, PA (R.J.L.).

Accompanying Data S1 and Figure S1 are available at <https://www.ahajournals.org/doi/suppl/10.1161/JAHA.117.007861>

*Dr Anselmo and Dr Branchetti contributed equally to this work.

Correspondence to: Giovanni Ferrari, PhD, Department of Surgery, Columbia University, Columbia University Vagelos College of Physicians and Surgeons, 630W 168th Street, Suite 15.401c, New York, NY 10032. E-mail: gf2375@cumc.columbia.edu

Received November 6, 2017; accepted July 27, 2018.

© 2018 The Authors. Published on behalf of the American Heart Association, Inc., by Wiley. This is an open access article under the terms of the Creative Commons Attribution-NonCommercial-NoDerivs License, which permits use and distribution in any medium, provided the original work is properly cited, the use is non-commercial and no modifications or adaptations are made.

Clinical Perspective

What Is New?

- Aortic valve sclerosis, the early presentation calcific aortic valve disease, is associated with pronounced architectural remodeling despite marginal effects on mechanical properties in both human and mice.
- MnTnBuOE-2-PyP⁵⁺ prevents aortic valve thickening in a murine model of aortic valve sclerosis.

What Are the Clinical Implications?

- Because this compound has been approved recently for clinical use for other indications, this work could shift the focus for the treatment of calcific aortic valve disease, moving from aortic valve stenosis to an earlier presentation (aortic valve sclerosis) that could be more responsive to medical treatment.

undergo replacement of the valve.^{12,13} Potential therapies are hampered by our poor understanding of the molecular mechanisms leading to AVSc and by the asymptomatic nature of its clinical presentation.

Although sclerotic valves are hemodynamically normal, valve interstitial cells (VICs) have already been activated and remodeling of the leaflet has begun.^{1,14–16} We and others have shown that an early pathological event in the remodeling of the AV is the accumulation of reactive oxygen species (ROS).^{14,17} ROS generates an oxidative injury that activates VICs with an impaired response to DNA damage in the sclerotic AV. In both humans and mice, impaired cellular responses to DNA damage are associated with premature aging and valve disease.¹⁸ A hallmark of this phenomenon is the sustained formation of subnuclear structures known as *DNA-repair foci*.¹⁴ We demonstrated that adenoviral delivery of antioxidant enzymes reverses ROS-induced DNA damage and reduces AVSc-derived VIC activation and calcification.¹⁴

Another key pathway in AVSc is the osteogenic differentiation induced by the TGF- β (transforming growth factor β) superfamily.^{15,19} We and others reported that mechanical stimulation and BMP4 (bone morphogenetic protein 4) are able to further differentiate VICs, with expression of extracellular matrix (ECM) regulators, such as osteopontin, CTGF (connective tissue growth factor), TSP (thrombospondin)-1 and -2, collagen, and osteocalcin, promoting valvular ectopic calcification.^{15,20,21} A BMP4 antagonist, Noggin, reverses this effect. The functional association of osteopontin with one of its receptors, CD44v6, contributes to the regulation of calcium deposition in vitro and ex vivo.¹⁶

Perhaps a major challenge in advancing our knowledge of AV disease is the lack of a reliable animal model to translate basic and clinical science data into an in vivo experiment.

Available models can develop calcification of the AV structures, but they rarely develop the large drop in pressure across the valve and other hemodynamically significant changes seen in human patients. We have shown that a lesion similar to human AVSc can be elicited in a mouse model given a hypercholesterolemic diet in combination with chronic infusion of Ang II (angiotensin II). Analyses of the aortic valve in these animals demonstrate ROS accumulation, cusp thickening, and ECM remodeling. This model does not mimic AS but rather resembles the early initiating phases of AVSc.

Oxidative damage to DNA is thought to contribute to a number of human pathologies. To modulate the oxidative response in vitro and ex vivo, a class of manganese porphyrin-based compounds have been identified. They are potent anti-inflammatory agents that catalytically inactivate a range of ROS and interact with transcription factors.^{22–25} An analog, MnTnBuOE-2-PyP⁵⁺ (MnBuOE),²⁴ is currently in early phase clinical trials (NCT02655601, NCT0338650, and NCT02990468) to mitigate the oxidative damage caused by radiation therapy.

We hypothesized that sclerotic AV leaflets, although normally functioning, are already biologically altered at both extracellular and cellular levels. To investigate this hypothesis, we pursued an experimental design that involved human aortic leaflet specimens, a murine model of AVSc, and a biomechanical simulator. The human biobanking efforts of 2 different institutions allowed us to compare explanted human AV leaflets from across the spectrum, from healthy to AVSc to AS. This work intends to provide an in-depth characterization of the early changes in the AV architecture, using histological, structural, and biomechanical analysis. We also tested the ability of the SOD (superoxide dismutase) mimic MnBuOE to control activation of human VICs in vitro and to reduce thickening of AV leaflets in a murine model. Because our SOD mimic MnBuOE has been approved recently for clinical trials, our work represents one of the first steps toward better understanding and eventually mitigating the pathogenesis of aortic valve degeneration.

Method

The authors declare that all supporting data are available within the article (and its online supplementary files).

Study Population and Patient Adjudication

Sclerotic aortic valves were collected from the explanted hearts of patients undergoing heart transplantation and from deceased donor hearts that were considered unsuitable for transplantation following institutional review board–approved guidelines of the University of Pennsylvania Perelman School of Medicine (protocol no. 809349), Columbia University

(AAAR6796), and the Valley Hospital (protocol no. 20132309). Informed consent was obtained for participant enrollment, and clinical information was obtained by patient interview and chart review. AVs from AS patients were collected from patients undergoing AV replacement, as described previously.^{14–16} Surgical patients were assessed by transesophageal echocardiography, computed tomography, or both and confirmed by intraoperative observation if applicable. AVSc has been defined by the American Heart Association and American College of Cardiology guidelines¹⁴ as focal areas of leaflet calcification with leaflet thickening. For this study, we defined AVSc as irregular, nonuniform thickening of portions of the AV leaflets or commissures or both, thickened portions of the AV with/without an appearance suggesting calcification (ie, bright echoes), nonrestricted or minimally restricted opening of the aortic cusps, and peak continuous-wave Doppler velocity across the valve <2 m/s.

In Vitro MnBuOE, MnE (MnTE-2-PyP5+), and TGF- β Treatment of VICs

Patients' derived cells were treated with 30 μ mol/L MnBuOE, 30 μ mol/L MnE (MnTE-2-PyP5+), and 10 ng/mL TGF- β and harvested 72 hours later for RNA and protein analysis. Gene expression level was standardized to actin B, and fold changes were calculated using untreated cells as basal.

Collagen Fiber Alignment

Small-angle light scattering was used to quantify collagen fiber architecture at different disease stages. Samples used for small-angle light scattering were shipped to the University of Texas (UT) Austin in PBS. After 2 PBS washes, the samples underwent a gradient glycerolization, as described previously.¹ Briefly, the fixed samples were dehydrated, cleared in a graded glycerol/water solution, and stored in 100% glycerol. A 5-mW nonpolarized continuous HeNe laser (JDS Uniphase Corp) was passed through the tissue samples, and the normalized orientation index (NOI) was used to quantify tissue deformation. The NOIs for each sample (nondiseased, sclerotic, and stenotic) were averaged and used to compute an average NOI representative of the collagen fiber architecture at each CAVD stage.

Microstructural Analysis

Scanning electron microscopy was used to characterize the microstructure of diseased AV leaflets in humans and mice. Samples were fixed in grade II EM-grade glutaraldehyde (Electron Microscopy Sciences) and shipped to UT Austin in fixative. Samples were stained with osmium tetroxide for 4 hours, critically point dried, and then cut to image the transmural/circumferential cross-section en face. Samples

were mounted on aluminum stubs, coated with carbon paint, sputter coated with 15 nm of Platinum/Palladium using a Cressington 208 Benchtop Sputter Coater, and imaged with a Zeiss Supra 40V scanning electron microscope (Carl Zeiss AG).

Quantification of Oxidized Amino Acid in the AV Explants

Thick paraffin sections (50 μ m) were used for oxidized amino acid (OxAA) analyses, as described previously.^{26,27} The content of each OxAA in paraffin-embedded AV leaflet samples was determined by stable isotope dilution liquid chromatography tandem mass spectrometry methods with an AB SCIEX API 5000 triple quadrupole mass spectrometer interfaced with an Aria LX Series HPLC multiplexing system (Cohesive Technologies Inc) in the Mass Spectroscopy Core Facilities of the Cleveland Clinic laboratories, as described.^{26,27} Briefly, samples were deparaffinized with xylene and mixed with a single-phase mixture of H₂O/methanol/H₂O-saturated diethyl-ether (1:3:8 vol/vol/vol) after protein delipidation and desalting. The mixture was then supplemented with synthetic [¹³C₆]-labeled OxAA standards and isotope-labeled precursor amino acids ([¹³C₉, ¹⁵N₁]-tyrosine and [¹³C₉, ¹⁵N₁]-phenylalanine). The mixtures were then hydrolyzed under argon gas using methane sulfonic acid and then passed through a C₁₈ solid-phase extraction column (Discovery DSC₁₈ mini-column, 3 mL; Supelco). During liquid chromatography tandem mass spectrometry, each OxAA and its precursor, tyrosine or phenylalanine, were quantitated, with results presented as a ratio of OxAA:tyrosine, the precursor amino acid.^{26,27}

Ang II Chronic Infusion Model

Seven-week-old wild-type male mice (C57BL/6J) were fed with a hypercholesterolemic diet and infused with saline or Ang II (1000 ng/kg per minute) using osmotic pumps (Alzet 2004) for 28 days, as described previously.^{14–16} In total, 28 treated and 12 untreated mice were used. Blood pressure measurements were performed in conscious mice using a computerized tail-cuff method (Coda 8; Kent Scientific Corp), as reported previously. Mice were euthanized with an inhalation overdose of isoflurane. AVs were harvested after 28 days. Experiments were conducted under the approved institutional animal care and use committee protocols 804440 (University of Pennsylvania) and AC-AAU6474 (Columbia University).

SOD Mimics Preparation

MnBuOE solution was diluted in water to obtain a concentration of 1 mmol/L. The solution was filtered and stored in a

sterile container. MnBuOE was administered by daily intraperitoneal injections at a concentration of 1 mg/kg for 2 days and then 0.5 mg/kg for up to 26 days. Another SOD mimic, MnE, was administered by daily intraperitoneal injections at a concentration of 10 mg/kg per day for the first 2 days and then with 5 mg/kg per day for 26 days.

Bioreactor Design and Tissue Preparation

The tension bioreactor used in this study is similar to the previously described flexure bioreactor used for flexural stimulation of engineered valve tissue, as described earlier.^{28,29} The bioreactor consists of 2 chambers, each with multiple media baths; each bath has stationary pins press-fit into the bottom for tissue anchorage. The opposing pins are fixed to an actuating arm that is attached to a cross-arm, which is connected to a central motorized piston. Intact human AVs excised in operating rooms were collected in Advanced DMEM and maintained at 4°C to ensure maximal cell survival during transport. Each leaflet was trimmed to form a tissue strip measuring 20 mm circumferentially and 8 mm radially. An attempt was made to keep endothelial cells viable through limited handling. The tissue strip was threaded into the springs and inserted into the tension bioreactor and used for the experiments.

Statistical Analysis

Quantitative data including age at surgery, calcium levels, and OxAA levels in AV leaflets were presented as mean±SE. Given the small sample size, nonparametric tests such as the Mann–Whitney test and the Kruskal–Wallis test (depending on the number of levels within the independent variable) were used to test differences between groups. Multiple comparisons were adjusted using Bonferroni correction. Statistical analyses were performed with R (version 3.4.2; R Foundation for Statistical Computing). $P \leq 0.05$ was considered significant.

Results

Human AV Sclerosis Is a Pathological But Reversible Stage of CAVD

Under approved institutional review board protocols, we created a collection of human AV cusps from patients undergoing open heart surgery or heart transplant (Table 1). Alizarin red was used to stain calcific deposits in histological sections and revealed minimal calcification of AVSc compared with AS (Figure 1A). Because altered ECM has been reported in AS, we used real-time reverse transcriptase–polymerase chain reaction and quantitative polymerase chain reaction to measure the expression levels of functional regulators of valve

architecture such as OPN (osteopontin), CTGF (connective tissue growth factor), Cyr61 (cysteine rich angiogenic inducer 61), osteonectin, TSP (thrombospondin)-1 and -2, and tenascin in human cusps from healthy control, AVSc, and AS tissues (n=5 per group). Figure 1B shows that the expression of these proteins increases in the asymptomatic stages of CAVD compared with healthy controls. We then used uniaxial biomechanical testing to confirm the plasticity of AVSc phase of CAVD with data showing that the expression of CTGF, OPN, and Cyr61 is induced by a combination of mechanical stimuli (15% stretch at 1 Hz, resembling the physiological cusp deformation) and osteogenic media (10 ng/mL of BMP4; Figure 1C through 1F), confirming our previously published data.^{10,14,16}

Architectural Remodeling of Collagen Fiber Orientation in Human AVSc

Histological analysis showed that AVSc is characterized by thickening of the cusps (Figure 2A). We measured the collagen fiber networks by picrosirius red staining, which confirms architectural remodeling of ECM in AVSc (Figure 2B). Collagen not only provides the AV tissue with its structural integrity but also affects cellular processes through matricellular, matricrine, and mechanical mechanisms.^{30,31} To examine how collagen fiber architecture is organized in different stages of the disease, human aortic valve specimens were fixed, optically cleared with glycerol, and examined with small-angle light scattering to measure the NOI of the collagen fibers at the different disease states (Figure 2C and 2D). As we predicted, collagen fibers are less aligned in the AVSc and AVS samples compared with the healthy control (nondiseased) tissue, as indicated by the average NOI, which drops from 34% in the healthy valve to 31% and 21% in the valves with AVSc and AS, respectively.

Table 1. Patient Demographics

Demographic	Control (n=16)	AVSc (n=18)	AS (n=23)
Age, y, mean±SE	62.5±1.9	65.6±1.3	73.6±5.18
Male	8 (50.0)	10 (55.5)	14 (60.8)
Smoker	2 (12.5)	7 (38.8)	6 (26.0)
Diabetes mellitus	3 (18.7)	2 (11.1)	3 (13)
Hypertension	5 (31.2)	10 (55.5)	15 (65.2)
Cerebrovascular accident	1 (4.4)
Peripheral vascular disease	1 (6.23)	1 (5.5)	2 (8.7)
Hyperlipidemia	8 (50.0)	7 (38.8)	7 (30.4)
CAD	4 (25.0)	6 (33.3)	5 (21.7)

Data are shown as n (%) except as noted. AS indicates aortic valve stenosis; AVSc, aortic valve sclerosis; CAD, coronary artery disease.

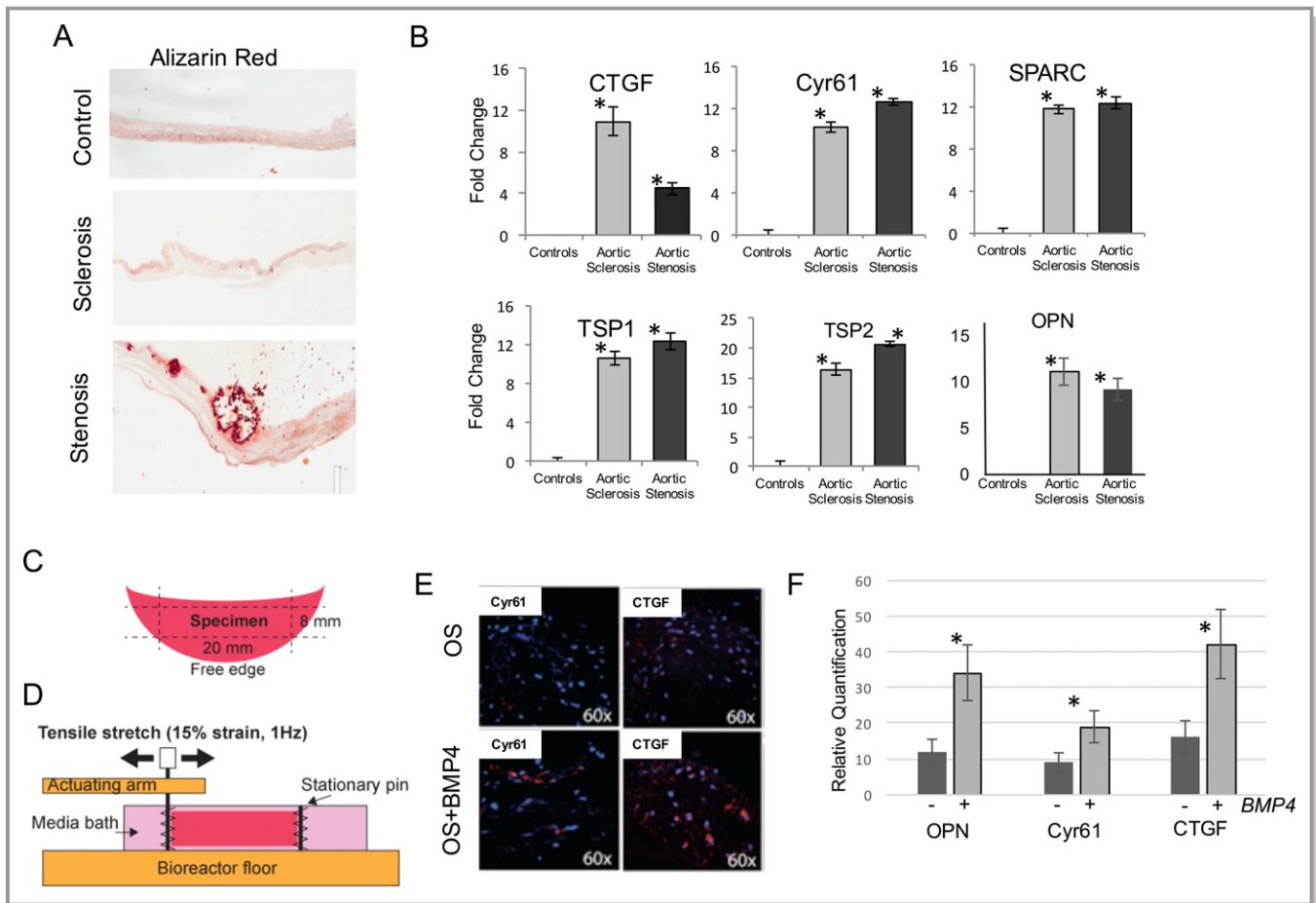


Figure 1. A, Alizarin red staining shows increased calcification in human sclerotic and stenotic aortic valves ($n=5$ per group). B, Bar graph shows fold-change gene expression of CTGF (connective tissue growth factor), Cyr61 (cysteine-rich angiogenic inducer 61), SPARC (secreted protein acidic and cysteine rich (osteonectin)), TSP (thrombospondin) -1 and -2, OPN (osteopontin) transcripts by reverse transcriptase–quantitative polymerase chain reaction (RT-qPCR). Data were normalized against 18S (actin B) gene expression and represented as fold change+SE. * P , 0.01 ($n=5$ per group). C and D, Tissue preparation and representation of tensile uniaxial bioreactor, respectively. E, Immunofluorescence staining showing expression of Cyr61 and CTGF in sclerotic aortic valve tissue cultured in static condition in the presence of OS (oscillatory shear stress) + BMP4 (bone morphogenetic protein 4) (100 ng/mL; $n=3$ per group). F, RT-PCR of OPN, Cyr61, and CTGF from RNA extracts collected from aortic valve cusps exposed to biomechanical stimulation (15% stretch at 1 Hz) for 6 days ($n=5$ per group). Osteogenic media enriched with BMP4 (100 ng/mL) was used.

Ultrastructural characterization of the VIC microenvironment via electron microscopy further highlights the disorganization of collagen fibrils already visible in AVSc (Figure 2E).

Products of Oxidative Modifications in AVSc and AS

Several pathological factors linked with abnormal mechanical stimuli have been shown to affect VICs and tissue structure. We investigated how the initiating events of AV remodeling affect AV cusp structure and mobility. We and others have reported extensively that ROS affects both collagen architecture and VIC activation.¹⁴ We showed that ROS accumulates in the early asymptomatic stages of CAVD (Figure 3A). With stable isotope dilution liquid chromatography tandem mass spectrometry, we

measured the accumulation of oxidized products in the explanted leaflets of 15 patients ($n=5$ per group; Tables 2 and 3). We found accumulation of dityrosine in end-stage disease (221 ± 41 $\mu\text{mol/mol}$ tyrosine), whereas other oxidized products were not significantly changed among the groups (Figure 3B and 3C). Univariate analysis of OxAA expression with the patients' comorbidities was performed. No significant association was noted except for dityrosine and comorbidities such as diabetes mellitus ($P=0.0014$) and hyperlipidemia ($P=0.019$; Table 4). Healthy and sclerotic AVs had no detectable levels of dityrosine. It is known that dityrosine, besides being an oxidation product, is also a crosslinker. Therefore, dityrosine crosslinking could increase cuspal stiffness and obstruction and thus contribute to ECM remodeling and calcium accumulation leading to impaired mobility typical of late stages of AV disease.

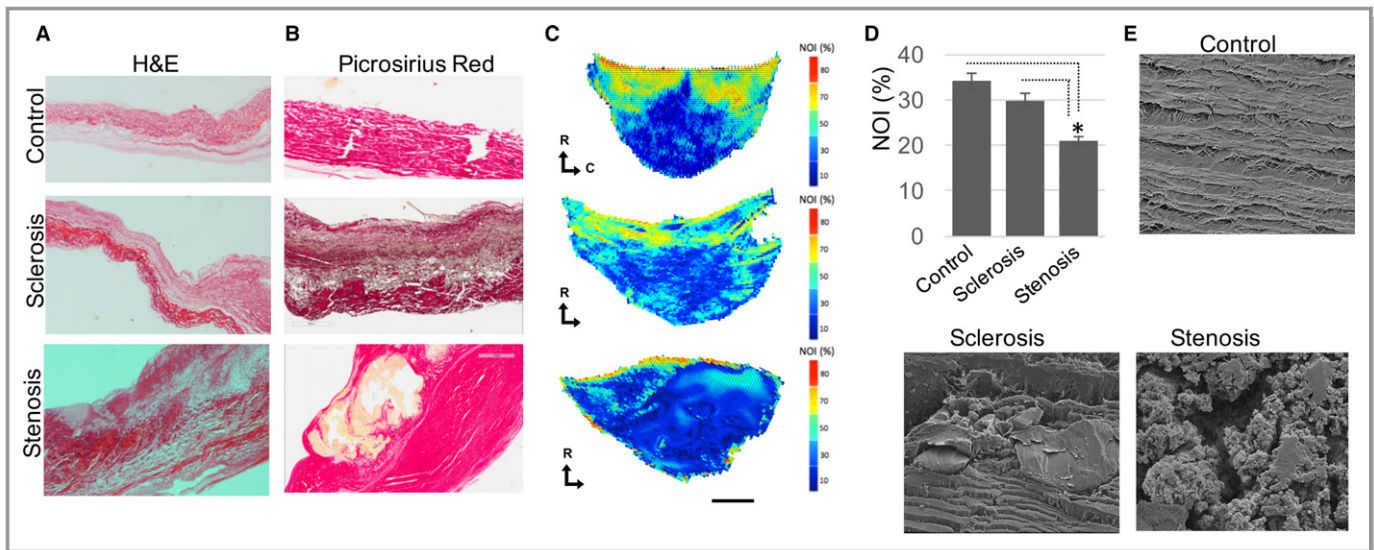


Figure 2. A, Hematoxylin and eosin (H&E) staining of human aortic valves (AVs) explanted from controls and from AV sclerotic and stenotic patients. B, Picrosirius red staining of control, sclerotic, and stenotic leaflets was visualized using brightfield microscopy and polarized light (n=5 per group). Collagen accumulation was detected in spongiosa and ventricularis areas in both sclerotic and stenotic valves. C, Collagen fiber alignment maps at control, sclerotic, and stenotic stages. Yellow and red represent highly aligned tissue (n=5 per group) (D). E, Scanning electron microscopy was used to show alteration in the microstructure of diseased AV leaflets (n=3 per group). NOI indicates normalized orientation index.

MnBuOE Controls Human VIC Activation and AV Thickening in a Murine Model of AVSc

ROS accumulation, such as superoxide products, can persist in injured tissues for years and have been widely associated with osteogenic differentiation.^{27–29} We reported that adenoviral transduction of antioxidant enzymes (SOD [superoxide dismutase] and CAT [catalase]) rescues VICs from an impaired DNA damage response by reducing the expression of early

markers of VIC activation and osteoblast-like differentiation.¹⁴ Figure 4A shows enhanced DNA damage response (γ -H2AX [γ -H2A histone family member X]) and osteogenic differentiation (RUNX2 [runt related transcription factor 2] and α -SMA [α -smooth muscle actin]) of human-derived aortic VICs from sclerotic patients under H₂O₂ treatment. There are, however, intrinsic limitations to adenoviral delivery in clinical therapy. Manganese porphyrins are a series of drugs that are catalytic scavengers of O₂⁻ and have been shown to have limited

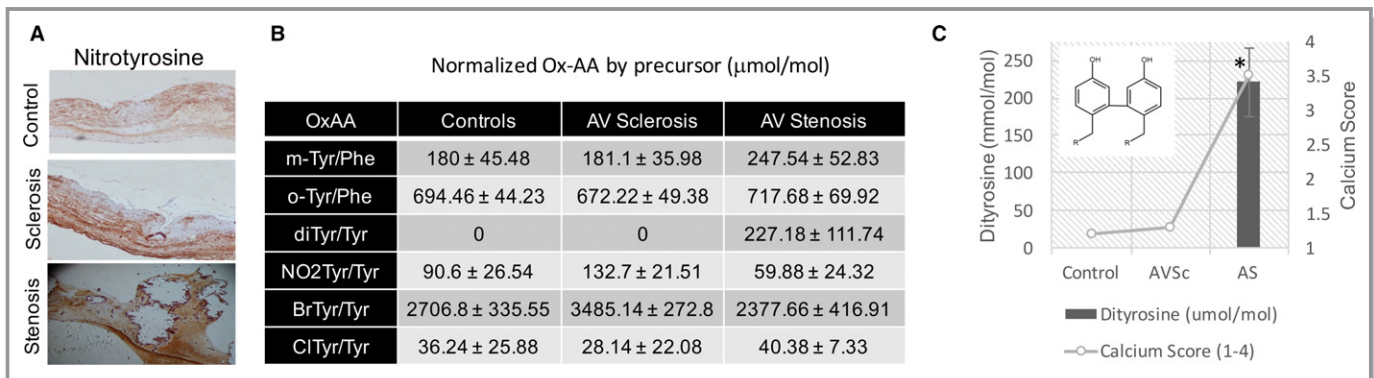


Figure 3. A, Immunohistochemical staining of control, sclerotic, and stenotic leaflets shows distribution of nitrotyrosine (NO₂Tyr) throughout leaflet, with areas of localized high-intensity staining in aortic valve (AV) sclerotic and stenotic tissues (n=5 per group). B, Oxidized amino acid (OxAA) quantification in explanted leaflets measured by liquid chromatography–tandem mass spectrometry and expressed as μmol/mol. C, Dityrosine (diTyr) quantification and calcium scores in control and AV sclerotic and stenotic leaflets. We conducted a Mann–Whitney U test to compare diTyr/tyrosine (diTyr/Tyr) in stenotic samples and controls (or sclerotic samples) and obtained a P value of 0.0075. BrTyr/Tyr indicates bromotyrosine/tyrosine; ClTyr/Tyr, Chlorotyrosine/tyrosine; diTyr/Tyr, dityrosine/tyrosine; m-Tyr/Phe, meta-tyrosine/phenylalanine; NO₂Tyr/Tyr, nitrotyrosine/tyrosine; o-Tyr/Phe, ortho-tyrosine/phenylalanine.

Table 2. Demographics of Patients for Stable Isotope Dilution LC-MS/MS

	Control	AVSc	AS
Patients, n	5	5	5
Age, y, mean±SE	36.17±9.44	63.67±6.17	77.91±5.17
Sex			
Male	1 (20)	2 (40)	1 (20)
Female	3 (60)	3 (60)	4 (80)
Unknown	1 (20)		
Ethnicity			
White	3 (60)	5 (100)	5 (100)
Black	1 (20)		
Not disclosed	1 (20)		
History of smoking	4 (80)	0	0
CAD	1 (20)	1 (20)	4 (80)
Diabetes mellitus	0	0	4 (80)
Hyperlipidemia	1 (20)	1 (20)	5 (100)
Hypertension	1 (20)	3 (60)	4 (80)

Data are shown as n (%) except as noted. AS indicates aortic valve stenosis; AVSc, aortic valve sclerosis; CAD, coronary artery disease; LC-MS/MS, liquid chromatography tandem mass spectrometry.

cytotoxicity. In this study, MnBuOE and MnE were used to prevent VICs from osteogenic differentiation in vitro measured by α -SMA. Figure 4B shows that MnBuOE prevents α -SMA upregulation induced by TGF- β , as a pro-osteogenic factor, on human-derived VICs.

We next tested the role of MnE and MnBuOE in controlling AV remodeling in vivo. Chronic infusion of Ang II in hypercholesteremic mice resulted in remodeling of the cardiac structures, including thickening of the heart valves.^{16,32} The choice of this animal model was driven by growing evidence indicating that Ang II induces its pleiotropic effects through

Table 3. OxAA Products From Stable Isotope Dilution LC-MS/MS

Diagnosis	m-Tyr/ Phe	o-Tyr/ Phe	diTyr/ Tyr	NO2Tyr/ Tyr	BrTyr/ Tyr	ClTyr/ Tyr
Control	0	649.5	0	0	2348.6	132.7
Control	210.7	704.8	0	115.5	2546	48.5
Control	215.6	602.6	0	63.3	3392.7	0
Control	224.7	859.1	0	127.2	1725.2	0
Control	249	656.3	0	147	3521.5	0
Sclerosis	75.2	596	0	87.4	3852.2	26.7
Sclerosis	137.6	707.8	0	93.7	3749.8	0
Sclerosis	270.4	519.2	0	178.2	4149.9	0
Sclerosis	249.9	774.7	0	189.9	2811.5	0
Sclerosis	172.4	538.4	0	114.3	2862.3	114
Stenosis	162.5	535.1	310.8	25.2	1468.5	13.4
Stenosis	435.4	959.1	630.2	28.5	1267.1	50.2
Stenosis	268.9	755.1	58.9	34.2	3041.2	44.3
Stenosis	236.1	677.6	93.4	56.9	3223.7	55.6
Stenosis	134.8	661.5	42.6	154.6	2887.8	38.4

LC-MS/MS indicates liquid chromatography tandem mass spectrometry; OxAA, oxidized amino acid.

NADPH-driven generation of ROS. Seven-week-old mice were fed a hypercholesteremic diet and infused with saline or Ang II using osmotic pumps for 28 days in the presence or absence of MnE or MnBuOE, as described in the Method section. Animals receiving chronic Ang II infusion showed increased thickening of the AV (Figure 4C–4G), prevented by cotreatment of ROS scavenger MnBuOE. Figure 4C shows the quantification of AV thickness in murine valves measured with hematoxylin and eosin staining (examples in Figure 4D). In Figure 4E, picrosirius red shows the impact of MnBuOE on collagen fiber. In contrast to these data, another manganese

Table 4. Univariate Analysis *P* Values of Relations Between OxAA Products and Clinical Comorbidities

	m-Tyr	o-Tyr	diTyr	NO2Tyr	BrTyr	ClTyr
Sex	0.3037	0.8392	0.9343	0.6354	0.9451	0.4263
Age	0.297	0.871	0.154	0.89	0.672	0.906
Smoking	0.4117	0.7531	0.1397	0.6608	0.2799	0.9462
Congestive heart failure	0.3048	0.4762	0.0856	0.3048	0.6857	0.2542
CAD	0.4894	0.104	0.0873	0.8513	0.2799	0.2002
Diabetes mellitus	0.9495	0.8513	0.0014*	0.2799	0.1773	0.2517
Hyperlipidemia	0.6126	0.7789	0.0192*	0.5358	1	0.2821
Hypertension	0.9551	0.3357	0.1905	0.8665	0.7789	0.232

CAD indicates coronary artery disease; OxAA, oxidized amino acid.
**P*<0.01.

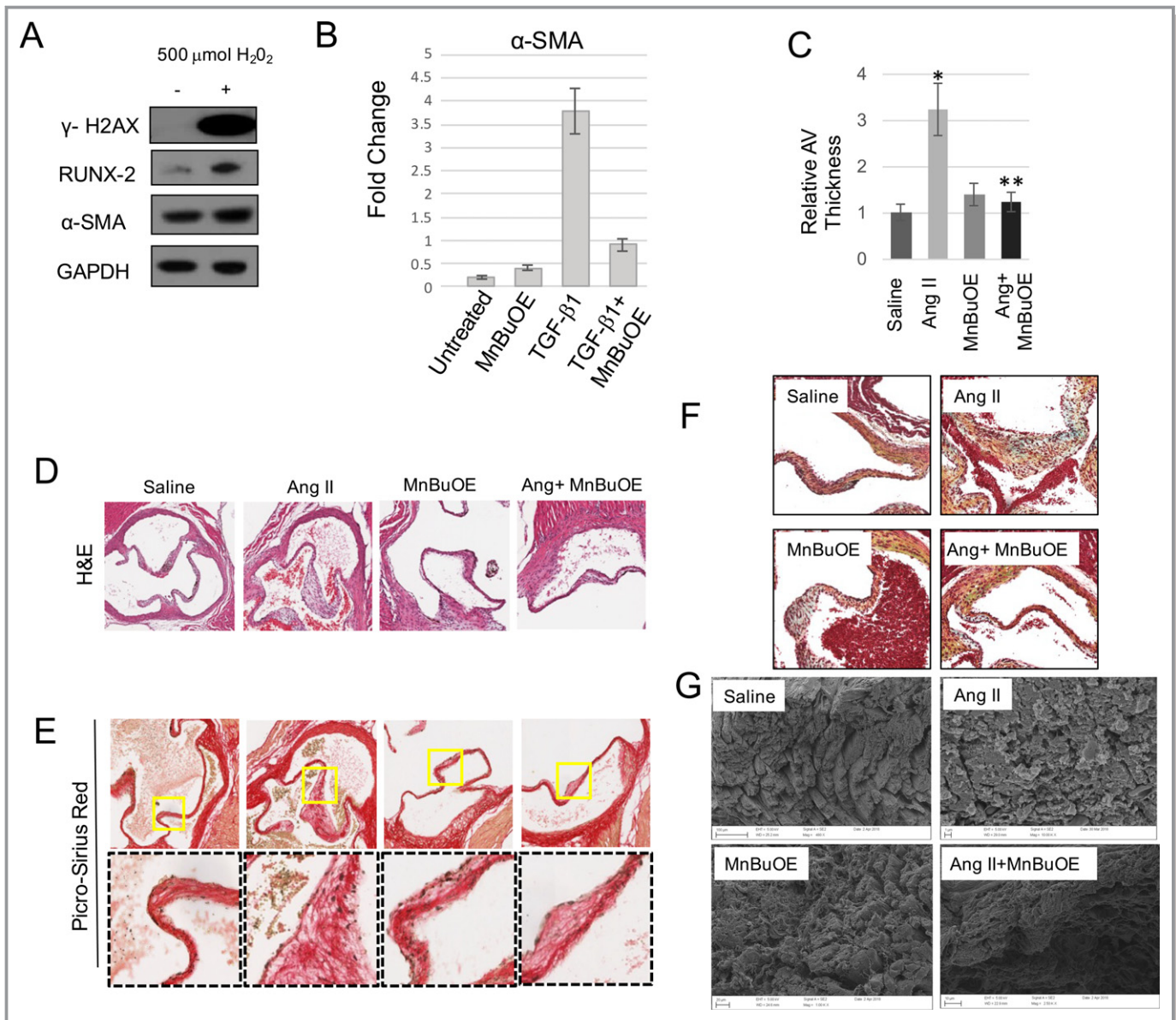


Figure 4. A, Western blot showing the expression of H2AX, RUNX2, and SMA (smooth muscle actin) in whole-cell extract of aortic valve (AV) sclerosis-derived valve interstitial cells treated or not with 500 $\mu\text{mol/L}$ of H_2O_2 . B, Bar graph shows fold-change gene expression of α -SMA evaluated by reverse transcriptase–quantitative polymerase chain reaction. Data were normalized against actin B and represented as fold change+SE. *Depicts statistically significant difference between Saline and Ang II ($P<0.01$). **Depicts statistically significant difference between Ang II+MnBuOE and Ang II ($P<0.01$). C, Relative AV thickness quantified using ImageJ with or without STDEV ($n=5$ per group) were used to evaluate differences in the thickness. D, Hematoxylin and eosin (H&E) staining of controls and AngII (angiotensin II) infused mouse AV tissues with or without MnBuOE or with MnBuOE alone. E, Collagen accumulation using picosirius red staining. F, Picosirius red staining of saline, Ang II, saline plus MnBuOE, and Ang II plus MnBuOE treated mice. G, Scanning electron microscopy used to show alteration in the microstructure of murine aortic valve leaflets.

porphyrin, MnE, although a potent SOD mimic, marginally mitigated valve remodeling (Figure S1A–S1C). Such data are likely due to the lower bioavailability of MnE to the tissues, cells, and cellular fragments than of MnBuOE. The log P_{ow} (the log value of the partition of the drug between *n*-octanol and water) was -7.79 for MnE and -4.10^{25} for MnBuOE.^{22,23,25}

Finally, we determined the impact of MnBuOE on murine valve ECM remodeling by both histological analysis and electron microscopy. Movat Pentachrome staining was performed on the murine AVs to evaluate the distribution and composition of the ECM. As shown in Figure 4F Ang II infusion induced thickening of the AV, which is characterized by significant ECM remodeling with abundant proteoglycan accumulation (blue

staining) and collagen deposition (yellow staining) distributed through the leaflet. Treatment with MnBuOE significantly prevents accumulation of both ECM components, with a stronger effect on collagen fibers deposition.

Ultrastructural characterization was also performed on explanted murine AV leaflets via electron microscopy. As shown in Figure 4G, collagen fibers are well defined and aligned in the murine AV leaflet of saline treated animals. Ang II infusion induced severe rearrangement of the leaflet and loss of fibril microstructure. Fiber disorganization was significantly reduced by treatment with SOD mimetics, and leaflet display improved collagen alignment compared with Ang II-treated AV.

Discussion

Our data show that AVSc is associated with profound architectural remodeling despite marginal effects on the mechanical properties of the valve *in vitro*. Our data support the theory that AVSc is an intermediate phase of the clinical progression from healthy to calcified AV. At the cellular level, the once-quiescent VICs found in a sclerotic AV have become activated and, given the right conditions, will continue to transdifferentiate into a new osteogenic phenotype. The tissue collected from AVSc patients was not calcified, which agrees with the normal hemodynamics of the valve. The tissue did, however, display expression patterns of functional regulators of valve architecture that were more consistent with end-stage CAVD. The central cusp deformation and dityrosine accumulation were suggestive of the additional mechanisms involved in early leaflet remodeling. Calcium deposition has an additive effect causing further cuspal stiffness and obstruction, contributing to ECM leaflet remodeling and impaired mobility. Further analysis of the microregional distribution of dityrosine and other cross-linkers could inform on the impact of these oxidative products on the ability of the AV to sustain deformation during each cardiac cycle. The *in vitro* testing in the bioreactor clearly demonstrated that in the presence of mechanical stimuli and osteogenic media, these activated VICs will continue their transdifferentiation into osteogenic-type cells. Interestingly, we found that the addition of a SOD mimic seemed to mitigate VIC activation. Treatment of human VICs with the manganese porphyrins prevented osteogenic differentiation *in vitro*. In the murine model, the administration of these SOD mimics prevents the thickening of AV leaflets, likely the result of a reduction in ECM.

AV degeneration is a long process with multiple stages. Clinically, we recognize AS as the most advanced form of the disease, with a clear impact on the hemodynamic performance of the valve. At that stage, the only form of therapy that resolves the problem is replacement of the diseased valve. Previous attempts to intervene in a nonsurgical or

nonpercutaneous fashion, including trials of statin therapy, have failed. The likely cause of that failure was not the form of therapy but rather the timing (ie, at the end of a calcific degenerative process). AVSc is a pathology that carries no hemodynamic consequences, but it is far from a benign state. It is a known risk factor for cardiovascular conditions such as congestive heart failure, myocardial infarction, and aortic valve pathology. In addition, our current work contributes to a growing body of literature that AVSc is a precursor to CAVD and suggests a new potential therapeutic window for the treatment of this condition.

Work by our group and others has suggested a possible role of oxidative products in the subclinical stages and progression of AV degeneration and remodeling. A correlation, for example, between PARP1 (poly[ADP-ribose] polymerase 1), a key regulator of oxidative DNA damage, and the progression of AS has been described. This process begins with events at the level of DNA. Our group has described the process of VIC transdifferentiation from a quiescent cell into an osteogenic-type cell, secondary to the effects of oxidative damage. This cellular transdifferentiation is accompanied by oxidative DNA damage manifested cytologically by the presence of a sustained DNA repair foci.

Our results also suggest that manganese porphyrins may inhibit the osteogenic transdifferentiation of VICs and reverse ECM remodeling. We used a variety of cellular and structural tools to identify and manipulate the mechanisms involved in early AV degeneration. These experiments helped us to better understand the different stages involved in the degeneration of AV leaflets and suggest that some of the structural changes may be reversible. Cationic Mn(III) porphyrins are among the most efficacious SOD mimics and redox-active experimental agents for the treatment of diseases associated with a disturbed cellular redox environment, commonly described as a state of oxidative stress.^{22,23,25,33} MnE was identified as a first powerful porphyrin-based SOD mimic with the safest toxicity profile.^{22,23,34,35} However, it was too hydrophilic and does not cross the blood–brain barrier to a sufficient extent. Indeed, the insufficient lipophilicity of MnE also resulted in its failure in our study. Further development resulted in the generation of MnBuOE,^{22–25,33,34,36} which accumulation in the brain justified its development as a radioprotector of normal brain. MnBuOE has been shown to act as a SOD mimic in several models, including mimicking the MnSOD isoform.^{22,23,25,35,37} In addition, it has been shown to upregulate MnSOD via activation of Nrf2 (Nuclear factor [erythroid-derived 2]-like 2).²⁴ The notable biological efficiency and the safe toxicity profile (eg, lack of genotoxicity in a rat Comet assay) of MnBuOE in preclinical studies have justified its adoption in clinical trials.³⁷ Such ability of Mn porphyrin-based SOD mimics may also be important in the field of heart valve biology, as the clinical management of cancer survivors after

exposure of mediastinal, thoracic, and breast radiotherapy has been influenced for many decades by major cardiovascular complications. In particular, thoracic radiotherapy is associated with a significant increase in valve pathology, with valve abnormalities appearing in 6% to 40% of Hodgkin lymphoma survivors.^{36,38–40} An initial important use of these compounds in cardiovascular medicine may lie in those patients who undergo radiation therapy for different types of malignancies, with the goal of limiting future radiotherapy-mediated DNA valvular injuries.

Several limitations are associated with this study. Despite our effort to create homogeneous patient profiles, our approach is based on human retrieved specimens from surgical cases. We have established a protocol to control patient adjudication (Data S1). Despite our efforts, there is intrinsic patient variability and heterogeneous comorbidities that could mask or highlight functional association between our molecular target and the patient profile. Another limitation is that in our bioreactor system, AV leaflets are stretched under uniaxial conditions rather than the more natural-mimicking biaxial conditions, but this was unavoidable under the current bioreactor setup.

This study helps to further our understanding of mechanisms of AV remodeling in AVSc and may have significant clinical implications. Patients may have AVSc for many years without any hemodynamic compromise of their valve, and this may represent a window of time when cellular changes could be reversed. We demonstrated the way in which one group of substances, a porphyrin-based SOD mimic recently approved for use in a clinical trial, could potentially prevent some mechanisms of AV remodeling. Additional work is needed, however, before this will be possible: First, we must find ways to measure subtle improvement and degeneration of sclerotic aortic leaflets. Echocardiography is not sensitive enough currently to accurately quantify minute changes in AV leaflets. Second, we must find a way to determine which subpopulation of patients with AVSc will go on to develop AS. The challenge we face now is to identify which patients are at risk for rapid evolution from AVSc to AS, as this will identify the target population for any future interventions. If we cannot determine which patients will develop AS and which patients will not progress beyond AVSc, we will be unable to identify the subpopulation that could most benefit from interventions at an early stage.

It is concluded that AVSc is associated with pronounced architectural remodeling despite marginal effects on the mechanical properties in both human and mice. MnBuOE prevents AV thickening in a murine model of AVSc. Because this compound has been approved recently for clinical use for other indications, this work could shift the focus for the treatment of CAVD, moving from AS to an earlier presentation (AVSc) that could be more responsive to medical treatment.

Acknowledgments

The authors thank Dr Suengwon Lee for his assistance with the murine model.

Sources of Funding

This work was supported by the following research grants and funds: National Institutes of Health (RO1-HL131872 to Ferrari and Levy, RO1-HL122805 to Ferrari), American Heart Association (grant 24810002 to Ferrari), the Kibel Fund for Aortic Valve Research (to Ferrari and Levy), the Valley Hospital Foundation “Marjorie C Bunnel” Charitable Fund (to Ferrari and Grau), and both Erin’s Fund and the William J. Rashkind Endowment of the Children’s Hospital of Philadelphia (to Levy).

Disclosures

Batinic-Haberle is a consultant with BioMimetix JVLLC and holds equities in BioMimetix JVLLC. IBH and Duke University have patent rights and have licensed technologies to BioMimetix JVLLC. The remaining authors have no disclosures to report.

References

- Gharacholou SM, Karon BL, Shub C, Pellikka PA. Aortic valve sclerosis and clinical outcomes: moving toward a definition. *Am J Med.* 2011;124:103–110.
- Yutzey KE, Demer LL, Body SC, Huggins GS, Towler DA, Giachelli CM, Hofmann Bowman MA, Mortlock DP, Rogers MB, Sadeghi MM, Aikawa E. *Calcific Aortic Valve Disease: A Consensus Summary From the Alliance of Investigators on Calcific Aortic Valve Disease.* Arteriosclerosis, Thrombosis, and Vascular Biology; 2014: Lippincott Williams & Wilkins; 2014:2387–2393.
- Linefsky JP, O’Brien KD, Katz R, de Boer IH, Barasch E, Jenny NS, Siscovick DS, Kestenbaum B. Association of serum phosphate levels with aortic valve sclerosis and annular calcification the Cardiovascular Health Study. *J Am Coll Cardiol.* 2011;58:291–297.
- Rajamannan NM, Evans FJ, Aikawa E, Grande-Allen KJ, Demer LL, Heistad DD, Simmons CA, Masters KS, Mathieu P, O’Brien KD, Schoen FJ, Towler DA, Yoganathan AP, Otto CM. Calcific aortic valve disease: not simply a degenerative process: a review and agenda for research from the National Heart and Lung and Blood Institute Aortic Stenosis Working Group. Executive summary: calcific aortic valve disease-2011 update. *Circulation.* 2011;124:1783–1791.
- Otto CM, Lind BK, Kitzman DW, Gersh BJ, Siscovick DS. Association of aortic-valve sclerosis with cardiovascular mortality and morbidity in the elderly. *N Engl J Med.* 1999;341:142–147.
- Cowell SJ, Newby DE, Prescott RJ, Bloomfield P, Reid J, Northridge DB, Boon NA; Scottish Aortic Stenosis and Lipid Lowering Trial, Impact on Regression (SALTIRE) Investigators. A randomized trial of intensive lipid-lowering therapy in calcific aortic stenosis. *N Engl J Med.* 2005;352:2389–2397.
- Parolari A, Tremoli E, Cavallotti L, Trezzi M, Kassem S, Loardi C, Veglia F, Ferrari G, Pacini D, Alamanni F. Do statins improve outcomes and delay the progression of non-rheumatic calcific aortic stenosis? *Heart.* 2011;97:523–529.
- Kapadia SR, Leon MB, Makkar RR, Tuzcu EM, Svensson LG, Kodali S, Webb JG, Mack MJ, Douglas PS, Thourani VH, Babaliaros VC, Herrmann HC, Szeto WY, Pichard AD, Williams MR, Fontana GP, Miller DC, Anderson WN, Akin JJ, Davidson MJ, Smith CR; Investigators PT. 5-year outcomes of transcatheter aortic valve replacement compared with standard treatment for patients with inoperable aortic stenosis (PARTNER 1): a randomised controlled trial. *Lancet.* 2015;385:2485–2491.
- Yutzey KE, Demer LL, Body SC, Huggins GS, Towler DA, Giachelli CM, Hofmann Bowman MA, Mortlock DP, Rogers MB, Sadeghi MM, Aikawa E. Calcific aortic valve disease: a consensus summary from the Alliance of Investigators on

- Calcific Aortic Valve Disease. *Arterioscler Thromb Vasc Biol.* 2014;34:2387–2393.
10. Grau JB, Poggio P, Sainger R, Vernick WJ, Seefried WF, Branchetti E, Field BC, Bavaria JE, Acker MA, Ferrari G. Analysis of osteopontin levels for the identification of asymptomatic patients with calcific aortic valve disease. *Ann Thorac Surg.* 2012;93:79–86.
 11. Sainger R, Grau JB, Branchetti E, Poggio P, Lai E, Koka E, Vernick WJ, Gorman RC, Bavaria JE, Ferrari G. Comparison of transesophageal echocardiographic analysis and circulating biomarker expression profile in calcific aortic valve disease. *J Heart Valve Dis.* 2013;22:156–165.
 12. Otto CM. Calcific aortic valve disease: new concepts. *Semin Thorac Cardiovasc Surg.* 2010;22:276–284.
 13. Towler DA. Molecular and cellular aspects of calcific aortic valve disease. *Circ Res.* 2013;113:198–208.
 14. Branchetti E, Sainger R, Poggio P, Grau JB, Patterson-Fortin J, Bavaria JE, Chorny M, Lai E, Gorman RC, Levy RJ, Ferrari G. Antioxidant enzymes reduce DNA damage and early activation of valvular interstitial cells in aortic valve sclerosis. *Arterioscler Thromb Vasc Biol.* 2013;33:e66–e74.
 15. Poggio P, Sainger R, Branchetti E, Grau JB, Lai EK, Gorman RC, Sacks MS, Parolari A, Bavaria JE, Ferrari G. Noggin attenuates the osteogenic activation of human valve interstitial cells in aortic valve sclerosis. *Cardiovasc Res.* 2013;98:402–410.
 16. Poggio P, Branchetti E, Grau JB, Lai EK, Gorman RC, Gorman JH, Sacks MS, Bavaria JE, Ferrari G. Osteopontin-CD44v6 interaction mediates calcium deposition via phospho-Akt in valve interstitial cells from patients with noncalcified aortic valve sclerosis. *Arterioscler Thromb Vasc Biol.* 2014;34:2086–2094.
 17. Heistad DD, Wakisaka Y, Miller J, Chu Y, Pena-Silva R. Novel aspects of oxidative stress in cardiovascular diseases. *Circ J.* 2009;73:201–207.
 18. Nagy E, Caidahl K, Franco-Cereceda A, Bäck M. Increased transcript level of poly(ADP-ribose) polymerase (PARP-1) in human tricuspid compared with bicuspid aortic valves correlates with the stenosis severity. *Biochem Biophys Res Commun.* 2012;420:671–675.
 19. Clark-Greuel JN, Connolly JM, Sorichillo E, Narula NR, Rapoport HS, Mohler ER, Gorman JH, Gorman RC, Levy RJ. Transforming growth factor-beta1 mechanisms in aortic valve calcification: increased alkaline phosphatase and related events. *Ann Thorac Surg.* 2007;83:946–953.
 20. Frangogiannis NG. Matricellular proteins in cardiac adaptation and disease. *Physiol Rev.* 2012;92:635–688.
 21. Okamoto H. Osteopontin and cardiovascular system. *Mol Cell Biochem.* 2006;300:1–7.
 22. Batinić-Haberle I, Tovmasyan A, Spasojević I. An educational overview of the chemistry, biochemistry and therapeutic aspects of Mn porphyrins—from superoxide dismutation to H₂O₂-driven pathways. *Redox Biol.* 2015;5:43–65.
 23. Batinić-Haberle I, Tovmasyan A, Roberts ERH, Vujaskovic Z, Leong KW, Spasojević I. SOD therapeutics: latest insights into their structure-activity relationships and impact on the cellular redox-based signaling pathways. *Antioxid Redox Signal.* 2014;20:2372–2415.
 24. Zhao Y, Carroll DW, You Y, Chaiswing L, Wen R, Batinić-Haberle I, Bondada S, Liang Y, St Clair DK. A novel redox regulator, MnTnBuOE-2-PyP⁵⁺, enhances normal hematopoietic stem/progenitor cell function. *Redox Biol.* 2017;12:129–138.
 25. Tovmasyan A, Sheng H, Weitner T, Arulpragasam A, Lu M, Warner DS, Vujaskovic Z, Spasojević I, Batinić-Haberle I. Design, mechanism of action, bioavailability and therapeutic effects of mn porphyrin-based redox modulators. *Med Princ Pract.* 2013;22:103–130.
 26. Lee S, Levy RJ, Christian AJ, Hazen SL, Frick NE, Lai EK, Grau JB, Bavaria JE, Ferrari G. Calcification and oxidative modifications are associated with progressive bioprosthetic heart valve dysfunction. *J Am Heart Assoc.* 2017;6:e005648. DOI: 10.1161/JAHA.117.005648.
 27. Christian AJ, Lin H, Alferiev IS, Connolly JM, Ferrari G, Hazen SL, Ischiropoulos H, Levy RJ. The susceptibility of bioprosthetic heart valve leaflets to oxidation. *Biomaterials.* 2014;35:2097–2102.
 28. Merryman WD, Youn I, Lukoff HD, Krueger PM, Guilak F, Hopkins RA, Sacks MS. Correlation between heart valve interstitial cell stiffness and transvalvular pressure: implications for collagen biosynthesis. *Am J Physiol Heart Circ Physiol.* 2006;290:H224–H231.
 29. Merryman WD, Liao J, Parekh A, Candiello JE, Lin H, Sacks MS. Differences in tissue-remodeling potential of aortic and pulmonary heart valve interstitial cells. *Tissue Eng.* 2007;13:2281–2289.
 30. Phillippi JA, Eskay MA, Kubala AA, Pitt BR, Gleason TG. Altered oxidative stress responses and increased type I collagen expression in bicuspid aortic valve patients. *Ann Thorac Surg.* 2010;90:1893–1898.
 31. Das D, Holmes A, Murphy GA, Mishra K, Rosenkranz AC, Horowitz JD, Kennedy JA. TGF-beta1-induced MAPK activation promotes collagen synthesis, nodule formation, redox stress and cellular senescence in porcine aortic valve interstitial cells. *J Heart Valve Dis.* 2013;22:621–630.
 32. Thalji NM, Hagler MA, Zhang H, Casacang-Verzosa G, Nair AA, Suri RM, Miller JD. Nonbiased molecular screening identifies novel molecular regulators of fibrogenic and proliferative signaling in myxomatous mitral valve disease. *Circ Cardiovasc Genet.* 2015;8:516–528.
 33. Rajic Z, Tovmasyan A, de Santana OL, Peixoto IN, Spasojević I, do Monte SA, Ventura E, Rebouças JS, Batinić-Haberle I. Challenges encountered during development of Mn porphyrin-based, potent redox-active drug and superoxide dismutase mimic, MnTnBuOE-2-PyP(5+), and its alkoxyalkyl analogues. *J Inorg Biochem.* 2017;169:50–60.
 34. Gad SC, Sullivan DW, Crapo JD, Spainhour CB. A nonclinical safety assessment of MnTE-2-PyP, a manganese porphyrin. *Int J Toxicol.* 2013;32:274–287.
 35. Rajic Z, Tovmasyan A, Spasojević I, Sheng H, Lu M, Li AM, Gralla EB, Warner DS, Benov L, Batinić-Haberle I. A new SOD mimic, Mn(III) ortho N-butoxyethylpyridylporphyrin, combines superb potency and lipophilicity with low toxicity. *Free Radic Biol Med.* 2012;52:1828–1834.
 36. Noël G, Mazon JJ. [Favourable and unfavourable effects on long-term survival of radiotherapy for early breast cancer: an overview of the randomised trials]. *Cancer Radiother.* 2001;5:92–94.
 37. Gad SC, Sullivan DW, Spasojević I, Mujer CV, Spainhour CB, Crapo JD. Nonclinical safety and toxicokinetics of MnTnBuOE-2-PyP5+ (BMX-001). *Int J Toxicol.* 2016;35:438–453.
 38. Heidenreich PA, Hancock SL, Lee BK, Mariscal CS, Schnittger I. Asymptomatic cardiac disease following mediastinal irradiation. *J Am Coll Cardiol.* 2003;42:743–749.
 39. Hull MC, Morris CG, Pepine CJ, Mendenhall NP. Valvular dysfunction and carotid, subclavian, and coronary artery disease in survivors of hodgkin lymphoma treated with radiation therapy. *JAMA.* 2003;290:2831–2837.
 40. Wethal T, Lund M-B, Edvardsen T, Fosså SD, Pripp AH, Holte H, Kjekshus J, Fosså A. Valvular dysfunction and left ventricular changes in Hodgkin's lymphoma survivors. A longitudinal study. *Br J Cancer.* 2009;101:575–581.

SUPPLEMENTAL MATERIAL

Data S1.

Supplemental Material and Methods

Patient Adjudication protocol. Correct patient adjudication is essential for any patient-oriented studies in human subject. Both biobanks have implemented mechanisms to ensure the accuracy of the research data associated with each specimen. These mechanisms are shared among the different institutions and are re-evaluated for improvement regularly. The valvular pathologies, with regards to the morphology of the valve, presence of calcium nodule thickening of the cusps, the degree of stenosis, and the etiology of the disease are assessed at the time of collection by the operating surgeon, via the echocardiographic reports at the Heart Transplant program and transcribed by the study staff from the original operative report or dictation into the research database. This is retrospectively re-assessed by cross-matching the entry in the biobank registry with the diagnosis entered in the pre-operative echocardiogram report as well as any ancillary imaging (e.g. CT scan, MRI). Any inconsistencies is adjudicated by the patient's operating surgeon or a qualified physician associated with the biobank. This adjudication includes a review of the operative report, pre- and peri-operative diagnostic imaging, and, where necessary, review of pathology reports. Clinical data, including pertinent medical history and comorbidities are extracted from the source (i.e. original hospital chart) and entered into the research database by trained study personnel, with regular auditing for quality and accuracy by the personnel involved using the patient's original medical record.

RT2 Profile PCR Array and RT-qPCR RNA was quantified using Nano drop and used for two step PCR amplification. 2 ug total RNA was converted into cDNA. cDNA was analyzed with the RT2 Profiler PCR Array for the detection of the expression of 84 human extracellular matrix and adhesion molecules. Real Time PCR (RT-qPCR) was performed on ABI Prism 7500 HT (Applied Biosystems, Carlsbad, CA), according to the manufacturer's instructions. Data analysis was performed using the web based qPCR data analysis software provided by SABiosciences. Validation of genes from PCR array was carried out by RT-qPCR using gene specific primers (OPN Fw 5'- TTG CAG CCT TCT CAG CCA A -3', Rv 5'- GGA GGC AAA AGC AAA TCA CTG -3'; THBS1 Fw 5'- CAC AGC TCG TAG AAC AGG AGG -3', Rv 5'- CAA TGC CAC AGT TCC TGA TG -3'; THBS2 Fw 5'- GCA GCG TCT CTG TGT TCT CA -3', Rv 5'- GAG TCA CTT CAG GGG TTT CG -3'; SMA Fw 5'-TTT TCC CAT CCA TTG TGG GAC-3', Rv 5'- TCC CAT TCC CAC CAT CAC C-3'; Cyr61 Fw 5'-CCC GTT TTG GTA GAT TCT GG-3', Rv 5'-GCT GGA ATG CAA CTT CGG-3'; SPARC Fw 5'-GAG AAA GAA GAT CCA GGC CC-3'; 18S Fw5'-GTAACC CGT TGA ACC CCA TT-3', Rv 5'-CCA TCC AAT CGG TAG TAG CG-3'. Dissociation curves were generated after each run to control formation of primer dimers. 18S gene expression was used for normalization. Normalization of each data point was carried out, in which $dCt = Ct(\text{test gene}) - Ct(18S)$; $ddCt = dCt(\text{test sample}) - dCt(18S \text{ control})$.

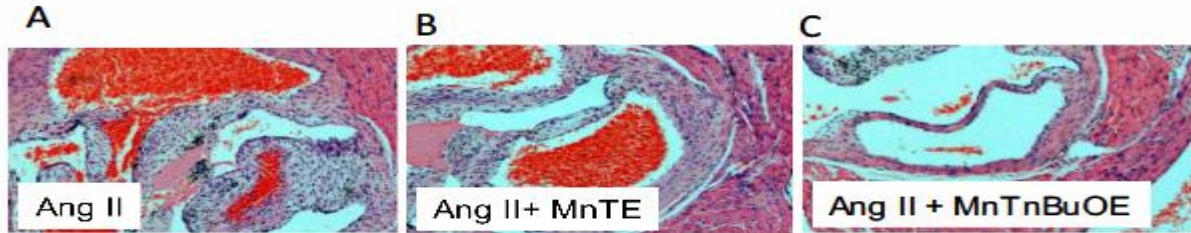
Histological analysis. Aortic valve tissues, Controls, Aortic valve Sclerotic (AVSc) and Aortic Valve Stenosis (AVS) were fixed in 10% Formalin and paraffin embedded. Hematoxylin & Eosin, Alizarin Red staining (for calcium) and Picrosirius Red (for collagen I and III fibers) were performed on 6 μ m sections by the Pathology Core of Children's Hospital of Philadelphia; Hematoxylin and Eosin (H&E), Alizarin Red staining (for calcium) was performed according to the protocol of the Histology Laboratory of the University Of Pennsylvania Perelman School of

Medicine. Picosirius red staining kit (ab150681) was performed on paraffin sections as described by the manufacturer (Abcam, Cambridge, UK).

Immunohistochemistry and Immunofluorescence Immunolocalization and expression of the proteins was demonstrated using specific antibodies against, CTGF (Ab6992), Osteopontin (Genway Biotech, San Diego, CA), SMA (Abcam, Cambridge MA), Periostin (Abcam, Cambridge MA), Cyr61 (Novus Biologicals, Littleton CO), GAPDH (ab9485) and, Nitrotyrosine (AB5411) from Millipore.

H₂O₂ treatment of VICs Primary human VICs were isolated and cultured from patients with Sclerotic and Stenotic aortic valves. Cells were cultured up to confluency and treated with 500 μ M H₂O₂ for 24 hours. After treatment cells were harvested for total RNA or protein isolation.

Figure S1. Seven-week-old wild type male mice (CS7BL/6J) were fed with hypercholesterolemic diet and infused with saline or Angiotensin II (1000 ng/kg/min) for 28 days.



MnTnBuOE-2-PypS+ and MnTE was administered by daily intraperitoneal injections. Animals subjected to chronic Ang II infusion show increased thickening of the AV (A), partially rescue by MnTE (B) or prevented by co-treatment of ROS scavenger MnBuOE (C).